

# Radiographic research of the Bi plasma jet formed by the vacuum arc discharge

A P Artyomov<sup>1</sup>, A G Roussikh<sup>1</sup>, A V Fedunin<sup>1</sup>, S A Chaikovskiy<sup>1,2</sup>, A S Zhigalin<sup>1</sup> and V I Oreshkin<sup>1</sup>

<sup>1</sup>Institute of High Current Electronics SB RAS, 2/3 Akademicheskoy Ave., Tomsk, 634033, Russia

<sup>2</sup>Institute of Electrophysics UD RAS, 106 Amundsen St., Ekaterinburg, 620016, Russia

E-mail: aap545@gmail.com

**Abstract.** The results of experiments on a soft x-ray radiography ( $\approx 1-2$  keV) of a bismuth plasma formed by the high-current vacuum arc discharge are represented. The plasma gun with the arc current  $\approx 60$  kA and the current rise time  $\approx 7$   $\mu$ s was used to produce the Bi plasma jet. The compact pulsed radiograph XPG-1 (250 kA, 220 ns) with an X-pinch load consisting of four Mo wires with a diameter 25  $\mu$ m was used as a source of the soft X-ray radiation. The X-ray backlighting images of the researched plasma jet and the Bi step-wedge with a step thickness of  $\approx 100$  nm were recorded simultaneously in the course of the experiment. A comparison of the plasma jet x-ray image with the current trace has enabled to estimate dependencies of the linear mass on the arc current. The experiments have shown that when the arc current density reaches  $\approx 3 \cdot 10^5$  A/cm<sup>2</sup>, the evaporation rate of the electrode material reaches  $\approx 100$   $\mu$ g/ $\mu$ s, that under the plasma velocity  $\approx 0.5$  cm/ $\mu$ s, provides a plasma jet linear mass  $\approx 200$   $\mu$ g/cm. At a distance of  $\approx 1-2$  mm from the arc cathode surface, the sharp increase of the jet linear mass (up to  $\approx 500$   $\mu$ g/cm) occurred.

## 1. Introduction

Currently, along with the Z-pinch based on the use of a wire array [1, 2] and a gas-puff [3, 4], Z-pinch based on the use of the vacuum arc discharge systems are employed [5 - 10]. The advantage of plasma liners based on arcs is that such a shell has not a problem with a "cold start", because their initial conductivity reaches significant values of  $\sim 10^4$  Ohm<sup>-1</sup>·m<sup>-1</sup> [11]. One of the most important parameters of the liner shell at the formation stage is the substance distribution (both radially and along its length). The most informative method for investigation of the dense plasma stream distribution is a soft X-ray radiography. The X-pinch high-temperature dense plasma was used as a radiation source for the X-ray radiography [12, 13, 14]. The X-ray radiography based on the X-pinch has a spatial resolution of 2-3  $\mu$ m, while a temporal resolution is about a nanosecond. The diagnostics, in a combination with the step-wedge manufactured from the same material as the investigated plasma, allows us to carry out not only a qualitative but also a quantitative analysis of the plasma flow structure. Knowledge of a distribution of the plasma flow linear mass is extremely important both for



the mathematical description of the Z-pinch implosion and a study of the fundamental laws of the electrodes material evaporation under the high current arc electrical discharge.

## 2. Experimental setup

The experiment was carried out on a special stand consisting of a plasma gun [5 - 10] (the arc current  $\approx 60$  kA and the current rise time  $\approx 7$   $\mu$ s) and a compact pulsed radiograph XPG-1 [12, 13, 14] (the current amplitude of 250 kA and a rise time of 220 ns). The plasma gun was used to form a bismuth plasma jet and the generator XPG-1 with the X-pinch load was used as a source of the soft X-ray radiation. The X-pinch load consisted of four Mo wires with a diameter 25  $\mu$ m. A drawing of the plasma gun is presented in figure 1. The plasma gun was fed by a capacitor bank with  $C = 20$   $\mu$ F which has been charged up to 20 kV. The bismuth cathode with a diameter of 5 mm was placed in a center of the plasma gun.

The experimental scheme with the soft x-ray radiography of a bismuth plasma jet is presented in figure 2. The scheme magnification is 1.48. In the experiment, a bismuth plasma image was registered using a Micrat-ORTO film. The photographic film was filtered by Kimfol 4 $\mu$ m +Al 0.4  $\mu$ m+ Polypropylene 6  $\mu$ m, to protect it from the exposure of arc self-radiation. Bismuth step-wedge with a step thickness of  $\approx 100$  nm was deposited on a polypropylene filter surface. Bismuth step-wedge was used to define a linear mass of Bi plasma produced by the vacuum arc.

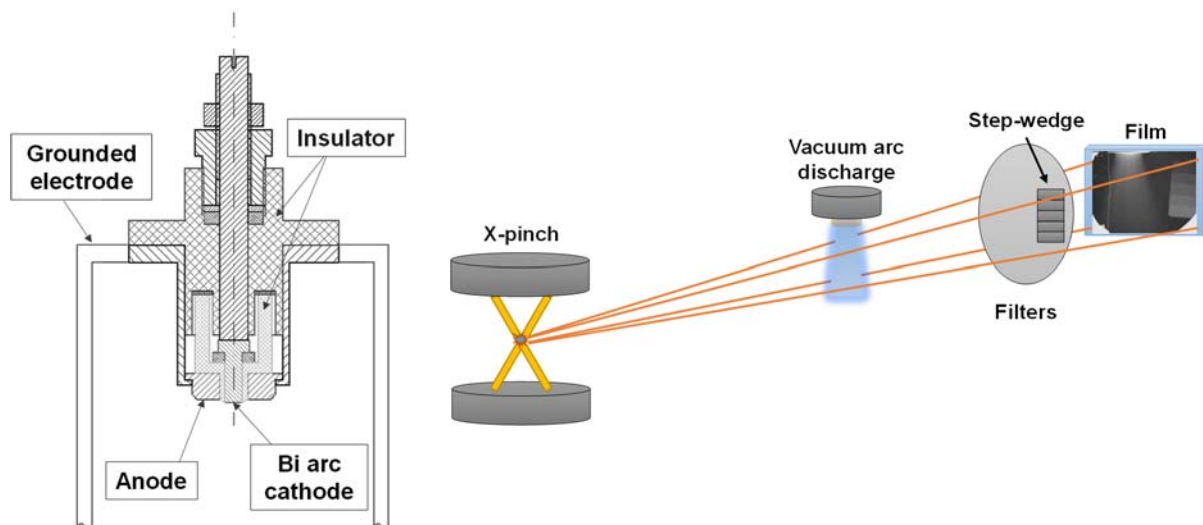


**Figure 1.** The drawing of plasma gun.

**Figure 2.** Sketch of soft x-ray radiography ( $\approx 1 \div 2$  keV) of a bismuth plasma jet formed by the high-current vacuum arc discharge.

The X-pinch and the plasma gun currents were measured with a Rogowski coil and a B-dot probe, correspondingly. The X-pinch x-ray emission was detected with a copper-cathode x-ray diode (XRD) filtered in the spectral region  $h\nu > 0.8$  keV.

Both generators were synchronized. We expect that the time of the maximum intensity of the substance evaporation must correspond to the maximum arc current. The X-pinch x-ray probing pulse occurred approximately at 1.5 - 2.0  $\mu$ s after the plasma gun current maximum. Such delay was chosen because of a substance with a maximum density needs some time to evaporate and fly a distance of about 1 cm, so that we were able to register it. Therefore, it was expected that the most contrast x-ray backlighting image would be registered at this time interval.

### 3. Experimental results

The main aim of the work was to determine the distribution of the bismuth plasma jet mass per unit length along the direction of jet propagation away from the cathode surface. For this purpose, in the experiments we recorded simultaneously two shadow images: 1 – bismuth plasma jet and 2 - bismuth step wedge. These images are presented in figure 3.

The step wedge image with an indicated thickness of steps is shown in figure 4. It is known that the optical density  $D$  is proportional to the radiation intensity  $I$ , transmitted through the test substance with the layer thickness  $h$ .

$$D \propto I \propto I_0 e^{-\mu \rho h}, \quad (1)$$

where  $\rho$  and  $\mu$  – the density and the absorption coefficient of the substance, through which the light passed. At the points, at which the optical density of the plasma  $D_{pl}$  and the optical density of one of the step wedge layer  $D_{sw}$  are the same, we can write the equation:

$$\rho_{pl} h_{pl} = \rho_{sw} h_{sw}, \quad (2)$$

where  $h_{pl}$  and  $\rho_{pl}$  - the thickness of the absorption layer and the averaged plasma layer density,  $h_{sw}$  and  $\rho_{sw}$  - the thickness and the density of the step wedge layer.

The registration of a shadow image of the bismuth step wedge allowed mathematically describe a direct relation between the value  $\rho_{sw} \cdot h_{sw}$  and the optical density  $D$ :

$$\rho h(D) = aD^2 + bD + c, \quad (3)$$

where the coefficients  $a$ ,  $b$ , and  $c$  depend on the intensity and the spectrum of a radiation source. Therefore, these coefficients should be determined for every image.

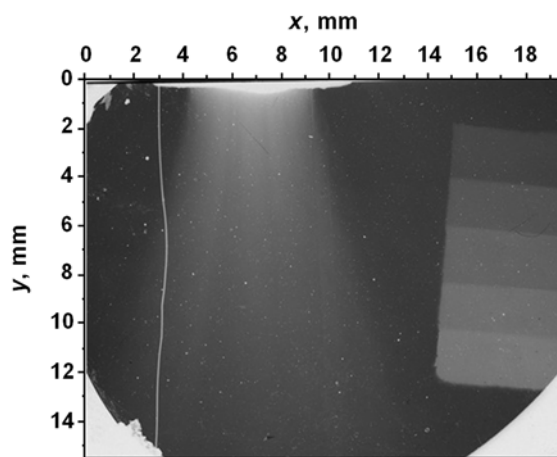


**Figure 3.** The Bi plasma and step-wedge backlight images.

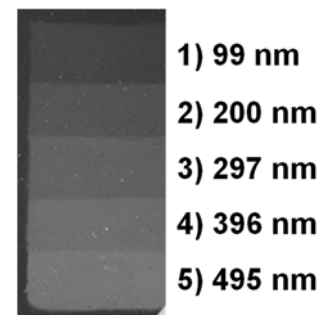


**Figure 4.** Step-wedge image with indicated thickness of steps.

The optical density distribution  $D(r)$  across the plasma jet image (the white lines in figure 5) was registered along the axis X (figure 3) in several cross-sections. Every cross-section was situated at some distance from the arc cathode. This distance to the cross-section corresponds to the time interval from the moment of evaporation of the cathode substance to the moment of image registration. Optical density distributions for several distances from the arc cathode are shown in figure 5. The thickness of every cross-section equals to 1 pixel of image. Therefore, dependences  $D(r)$  on the various distances from the arc cathode were used to study the dynamics of the arc plasma linear mass changes. In the experiments, the distance from the X-rays source to the investigated plasma jet is much greater than the jet diameter. Therefore, the incident radiation to the object under study can be approximately regarded as a flat, and the radiation absorbing layer depth at every point of the plasma jet radius is equal to the chord length at this point.

Using (3), we can plot the distribution of the  $h_{pl} \rho_{pl}$  value as a function of the cross section radius. The examples of  $h_{pl} \rho_{pl}$  distributions, as a function of  $r$ , that are built for the cross sections located at various distances from the cathode are shown in Figure 5.

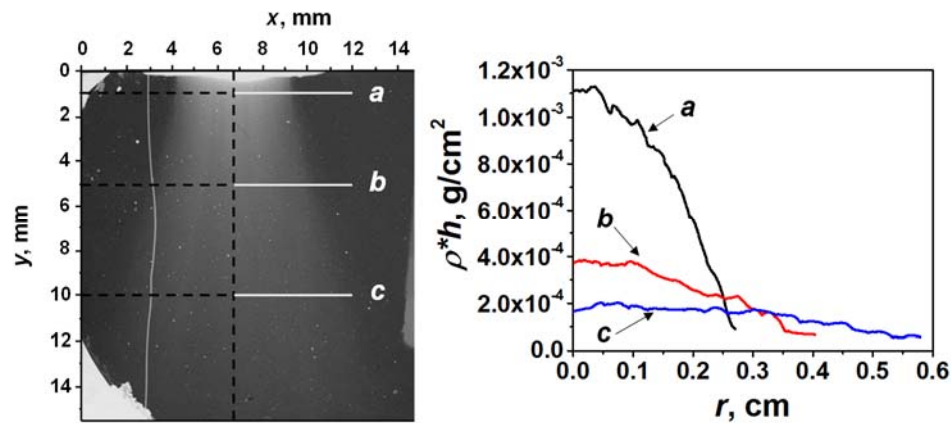


**Figure 5.** The multiplication of the plasma density and the radiation absorbing layer depth distribution  $h_{pl} \rho_{pl}$  as a function of radius  $r$  for several cross-sections located in various distances from the cathode.

The linear mass of an every plasma layer was calculated by integrating the multiplication of the density and the radiation absorbing layer depth along the radius:

$$m_p = 2 \int_0^R \rho \cdot h(r) dr. \quad (4)$$

The resulting set of the linear mass values for the cross sections located at various distances from the cathode surface allowed to estimate the dynamics of the linear mass evolution in time (see green points in figure 6). In order to determine the relationship between the distance from the arc cathode and the timeline, in this work we used the bismuth ions velocity equal to  $0.5 \text{ cm}/\mu\text{s}$  (for the arc current of 500 A), obtained in [15]. Traces of the vacuum arc current (black trace), the XPG-1 current (red trace), and the XRD signal (blue trace) are presented in figure 6 for comparison.

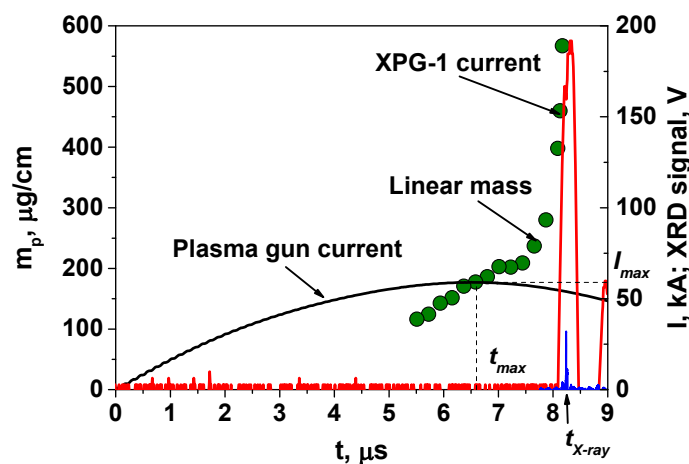


**Figure 6.** Dependence of the linear mass on time (green points) with traces of arc current (black), XPG-1 current (red) and XRD signal (blue).

#### 4. Conclusion

The experiments have shown that when the arc current density reaches  $\approx 3 \cdot 10^5$  A/cm<sup>2</sup>, the evaporation rate of the electrode material reaches  $\approx 100$   $\mu\text{g}/\mu\text{s}$ , that under the plasma velocity  $\approx 0.5$  cm/ $\mu\text{s}$  provides a plasma jet linear mass  $\approx 200$   $\mu\text{g}/\text{cm}$ . At a distance of  $\approx 1 - 2$  mm from the arc cathode surface, the sharp increase of the jet linear mass (up to  $\approx 500$   $\mu\text{g}/\text{cm}$ ) occurred.

This experimental fact can be explained in two different ways. The first explanation is that when the arc current density exceeds the some threshold value, the evaporation process begins to acquire an explosive character. Another explanation is the presence of molten metal droplets near the surface of the arc cathode. To clarify this experimental fact, it is necessary to carry out further studies of this physical phenomenon.

#### Acknowledgments

This work was supported in part by the Russian Foundation for Basic Research (grant No.15-08-03845-a and No. 14-02-00382-a)

#### References

- [1] Mazarakis M G *et al* 2009 *Phys. Rev. E.* **79** 016412
- [2] Aleksandrov V V, Barsuk V A, Grabovski E V, Gritsuk A N, Zukakishvili G G, Medovshchikov S F, Mitrofanov K N, Oleinik G M and Sasorov P V 2009 *Plasma Phys. Rep.* **35** 200
- [3] Coverdale C A *et al* 2010 *High Energy Density Physics* **6** 143
- [4] Coverdale C A *et al* 2007 *Phys. Plasmas* **14** 022706
- [5] Rousskikh A G, Shishlov A V, Zhigalin A S, Oreshkin V I, Chaikovskii S A and Baksht R B 2011 *Plasma Sources Sci. Technol.* **20** 035011
- [6] Rousskikh A G, Zhigalin A S, Oreshkin V I, Chaikovskiy S A, Labetskaya N A and Baksht R B 2011 *Phys. Plasmas* **18** 092707
- [7] Baksht R B, Rousskikh A G, Zhigalin A S and Oreshkin V I 2013 *IEEE Trans. on Plasma Sci.* **41** 1
- [8] Rousskikh A G, Zhigalin A S, Oreshkin V I, Labetskaya N A, Chaikovskiy S A, Batrakov A V, Yushkov G Yu and Baksht R B 2014 *Phys. Plasmas* **21** 052701
- [9] Rousskikh A G, Oreshkin V I, Zhigalin A S, Chaikovskiy S A, Baksht R B and Mitrofanov K N 2015 *Journ. of Phys.: Conf. Series* **652** 012065
- [10] Rousskikh A G, Zhigalin A S, Oreshkin V I, Frolova V, Velikovich A L, Yushkov G Yu and Baksht R B 2016 *Phys. Plasmas* **23** 063502
- [11] Rousskikh A G, Oreshkin V I, Zhigalin A S and Yushkov G Yu 2016 *Tech. Phys. Lett.* **42** 223
- [12] Ratakhin N A, Fedushchak V F, Erfort A A, Zharova N V, Zhidkova N A, Chaikovskii S A and Oreshkin V I 2007 *Rus. Phys. J.* **50** 193
- [13] Artyomov A P, Fedyunin A V, Chaikovskiy S A, Zhigalin A S, Oreshkin V I, Ratakhin N A and Rousskikh A G 2013 *Instr. Exp. Tech.* **56** 66
- [14] Baksht R B, Rousskikh A G, Zhigalin A S, Oreshkin V I and Artyomov A P 2015 *Phys. Plasmas* **22** 103521
- [15] Bugaev A S, Gushenets V I, Nikolaev A G, Oks E M and Yushkov G Y 2000 *Technical Physics.* **45** 1135